Wear Performance of The Zirconia Toughened Alumina Added With TiO_2 and Cr_2O_3 Ceramic Cutting Tool

Raqibah Najwa Mudzaffar
International Islamic University Malaysia
Mohamad Faiz Izzat Bahauddin
International Islamic University Malaysia
Hanisah Manshor
International Islamic University Malaysia
Ahmad Zahirani Ahmad Azhar
International Islamic University Malaysia
Nik Akmar Rejab
Universiti Sains Malaysia
Afifah Mohd. Ali (afifahali@iium.edu.my)
International Islamic University Malaysia https://orcid.org/0000-0003-2617-2540

Research Article

Keywords: ZTA, TiO2, Cr2O3, tool wear, ceramic tool

Posted Date: October 12th, 2021

DOI: https://doi.org/10.21203/rs.3.rs-956224/v1

Abstract

The zirconia toughened alumina enhanced with titania and chromia (ZTA-TiO_2-Cr_2O_3) ceramic cutting tool is a new cutting tool that possesses good hardness and fracture toughness. However, the performance of the ZTA-TiO_2-Cr_2O_3 cutting tool continues to remain unknown and therefore requires further study. In this research, the wearing of the ZTA-TiO_2-Cr_2O_3 cutting tool and the surface roughness of the machined surface of stainless steel 316L was investigated. The experiments were conducted where the cutting speeds range between 314 to 455 m/min, a feed rate from 0.1 to 0.15 mm/rev, and a depth of cut of 0.2 mm. A CNC lathe machine was utilised to conduct the turning operation for the experiment. Additionally, analysis of the flank wear and crater wear was undertaken using an optical microscope, while the chipping area was observed via scanning electron microscopy (SEM). The surface roughness of the machined surface was measured via portable surface roughness. The lowest value of flank wear, crater wear and surface roughness obtained are 0.044 mm, 0.45 mm^2, and 0.50 μm, respectively at the highest cutting speed of 455 m/min and the highest feed rate of 0.15 mm/rev. The chipping area became smaller with the increase of feed rate from 0.10 to 0.15 mm/rev and larger when the feed rate decrease. This was due to the reduced vibrations at the higher spindle speed resulting in a more stable cutting operation, thereby reducing the value of tool wear, surface roughness, and the chipping area.

1. Introduction

Ceramic cutting tools have been widely used as the preferred cutting tool [1] for the past century and continue to be used for machining in hard and difficult to cut materials such as alloy steel [2]. The reasons are because of their outstanding properties, such as wear resistance, shock resistance, and high hot hardness [3–9]. Moreover, alumina (Al_2O_3) based cutting tools are the most frequently used ceramics in machining hard materials [7–8] and have been a desirable choice to improve the quality of products and minimise the costs of manufacturing and production time [10]. This is due to its unique intrinsic properties, ideal for the cutting tool [11]. Additionally, it possesses high hardness, high wear resistance, and excellent abrasion resistance [5, 12]. However, alumina-based cutting tools are vulnerable to thermal cracking [13]. As such, zirconia (ZrO_2), is added to Al_2O_3 to form zirconia toughened alumina (ZTA) [14–17]. ZTA is known to be more affordable and eases the fabrication process [13]. Also, given its advantageous mechanical properties, it is commonly recognised as a tool material having high hardness, high-temperature strength, and able to sustain the shape of the cutting edge at higher temperatures [15]. In order to enhance ZTA's properties, such as fracture toughness and hardness, the additives are introduced into the ceramic compositions [18–19].

One of the additives used in this research is titania (TiO_2), given some reports stating that the sintering temperature of ZTA ceramic materials was scarcely maintained and achieved [20]. Indeed, with the addition of TiO_2, the sintering temperature of alumina can be reduced [21]. Despite that, TiO_2 also improved the sample's mechanical properties in providing resistance to abrasive wear and high-

temperature erosion corresponding to high thermal shock resistance [15]. Furthermore, a research study stated that the density value increased as Vickers hardness increased due to the addition of TiO_2 as an additive [22]. However, further addition of TiO_2 resulted in a minor increment of the values mentioned, where the value of the density is directly related to the Vickers hardness [21]. The highest bulk density, flexural strength, and hardness can be achieved with the combination of ZTA - 4% TiO_2 [22]. It is also found that the growth of the grain in the ZTA-TiO_2 composition was suppressed by the TiO_2 grain refiner up to 4% of TiO_2 addition and increases when the value exceeds 4%.

Furthermore, chromia (Cr_2O_3), is also used as an additive and has attracted increasing attention given its great ability to replace coated carbide or carbide itself [16]. Also, due to the addition of Cr_2O_3, grain growth can be observed in the optimum state. The density, fracture toughness, and Vickers hardness value of the sample also increased. This finding is supported by a study where the highest value could be obtained by adding 0.6 wt.% amount of Cr_2O_3 [15]. The author also mentioned that the interaction between the crack and the matrix grains improved by creating large plate-like grains. The strength increased due to grain deflection caused by the inter-granular fracture mode where cracks were dispersed along the grain's borders. Moreover, the isovalent solid solution is developed due to the composition of the chromia doped in alumina [12], mainly because both are in a similar corundum crystal and sesquioxides. Additionally, the Cr_2O_3 additives also affected the microstructure of ZTA due to the larger grains and resulted in the increment of fracture toughness.

During the machining process, the ceramic cutting tool undergoes fracture, cracking, and ladder-like chipping due to low toughness [23–25]. Therefore, for improved performance, a fabricated cutting tool can be accomplished by compacting the specific composition of ceramic powders with other reinforced materials [26]. However, the lack of toughness and high brittleness of the Al_2O_3 cutting tool can cause premature chipping at the edge of the tool [27–29]. Research of the microstructure and optimisation of machining parameters for ZTA-Cr_2O_3 has been reported by evaluating the composition's hardness and fracture toughness [16]. This combination can perform at high cutting speed and has excellent ability to replace coated carbide or carbide. However, even though the good properties of ZTA-TiO_2-Cr_2O_3 have been reported, the performance of the ZTA-TiO_2-Cr_2O_3 cutting tool remains unknown and requires further study. In addition, a detailed study on the wear of this cutting tool is needed to demonstrate and prove the performance of the tool.

Accordingly, this research focuses on the newly developed cutting tool, ZTA added with TiO_2 and Cr_2O_3. As such, the wearing of the ZTA-TiO_2-Cr_2O_3 cutting tool and the surface roughness on the workpiece surface will be examined in this research. Three types of tool wear were analysed, and the surface roughness of the machined surface, determined by the Ra value. It is anticipated that this study will contribute and extend previous research by developing a ceramic cutting tool in the steel cutting industry.

2. Material And Methods

In performing this experiment, alumina (Al_2O_3), yttria-stabilised zirconia (YSZ) at the ratio of 80:20 wt% were mixed with 3.0 wt% titania (TiO_2), and 0.6 wt% chromia (Cr_2O_3) additive materials. The weighted raw materials powders were prepared by wet mixing and set to 100 rpm for 24 hours utilising a Lab Roll ball mill (QM-5). After mixing for 24 hours, the mixture was placed into a glass beaker and dried in a Contherm drying oven (Thermotec 2000) for 24 hours at 100 ^oC. Next, the dried mixture was crushed by using agate mortar until it turned into powder. A weighing scale (AND FK-300i) was used to weigh 1 gram of the dried mixture powder before combining with a binder, polyethene glycol 400 mol. The mixed powder was then placed into a round mould, where manual compaction was performed using the uniaxial hydraulic hand press (Carver) to produce a round-pressed 13 mm diameter samples. The pressure of 100 MPa was applied and maintained for two minutes before removing the mould. The compacted samples were arranged on a tray and dried in the oven for 24 hours at 50 ^oC. The samples were sintered using the Yudian Muffler furnace at 1600^oC with 1 hour soaking time. The heating and cooling rate had been set to 5 ^oC/min.

The properties of the ZTA-TiO_2-Cr_2O_3 ceramic cutting tools were measured and shown in Table 1. The fabricated cutting tool is shown in Fig. 1. The turning process was performed using a CNC lathe machine (Bridge Port-Romi Powerpath) with a ZTA-TiO_2-Cr_2O_3 cutting tool mounted on a Sandvik Coromant (CRDNN 2525M 09-ID) tool holder. The machining was performed on stainless steel 316L at the parameters shown in Table 2.

Table 1
Properties of ZTA-TiO_2-Cr_2O_3 cutting tool

Properties	Value
Firing Shrinkage	16.29 %
Bulk density	4.09 g/cm^3
Vickers hardness	1394.41 HV
Fracture toughness	10.36 MPa.$m^{1/2}$

Table 2
Cutting parameter for ZTA-TiO_2-Cr_2O_3 cutting tool

Parameter	Condition/Value
Cutting Speed (m/min)	314, 361, 408, 455
Feed Rate (mm/rev)	0.1, 0.13, 0.15
Depth of Cut (mm)	0.2
Cutting Condition	Dry

Three types of wear analysis performed after the machining process which are flank wear, crater wear and chipping. Flank wear and crater wear was captured under an optical microscope (NIKON MM-4001L). The length of the flank wear was measured directly on the optical microscope as presented in Fig. 2.

Crater wear area on the other hand analyzed by using MATLAB programming software. The software measured the highlighted area to determine the crater wear area as shown in Fig. 3. Scanning electron microscopy (SEM) (JEOL JSM-IT100) was utilised to observe the chipping area on the ZTA-TiO_2-Cr_2O_3 cutting tool. The surface roughness of the machined surface, stainless steel 316L was measured by using the portable surface roughness (Mahr MarSurf M3000C). Three readings of surface roughness (Ra) were taken based on each machining parameter, and the average of the readings calculated.

3. Results And Discussion

3.1 Flank Wear

The graph of flank wear versus cutting speed at different feed rates illustrated in Fig. 4. Based on the graph, the flank wear trend decreases to about 72–80% when the cutting speed is increased from 314 to 455 m/min. The same trend can be seen for the feed rate in Fig. 5 where the decrement between 41–70% in flank wear value occurred due to the increment in feed rate from 0.10 to 0.15 mm/rev. Additionally, the highest value of flank wear obtained for the ZTA-TiO_2-Cr_2O_3 ceramic cutting tool is 0.655 mm at the lowest cutting speed of 314 m/min and the lowest feed rate of 0.10 mm/rev. The lowest value of flank wear acquired for the ZTA-TiO_2-Cr_2O_3 ceramic cutting tool is 0.044 mm at the highest cutting speed of 455 m/min and the highest feed rate of 0.15 mm/rev.

The example of flank wear observations are presented in Fig. 6 showing the effect of cutting speed to the the flank wear while Fig. 7 presenting the flank wear observed with the increment of feed rate.

These result can be supported by a study in [8] where the flank wear decreased with the increment of cutting speed. This was due to the reduced vibrations at the higher spindle speed resulting in a more stable cutting operation, thereby reducing the flank wear of the cutting tool [11]. The grain size difference in the alumina cutting tool is also one of the factors that could affect the value of the flank wear [30]. The finer grain size of the cutting tool will provide higher resistance to wear once the compacted powder is mixed with the other materials [12]. Besides, a lower temperature is generated with the cutting speed of 314 m/min than the temperature at 455 m/min during the turning process. However, having said that, the low temperature is not adequate to soften the steel. Thus, it would be difficult to cut the workpiece and resulting in a high cutting force that leads to high flank wear [31].

The selection of the cutting parameters can also influence the rate of tool wear. For instance, research shows the effects of machining parameters on tool wear during machining AISI 4340 steel with coated carbide tools [32]. The increment of the tool wear is almost linearly when the cutting speed and feed rate increase. An increasing trend of flank wear can also be observed when the cutting speed increases.

However, the flank wear decreases with the feed rate of 0.2 mm/rev and slightly increases when the feed rate is increased to 0.3 mm/rev. This occurred because of the abrasion by rubbing the flank surfaces at lower temperatures. Also, the effect of the cutting speed on the flank wear rate is revealed in a study where the wear rate decreased at the beginning of the test, and the value maintained during 200 m/min until the last run [8]. The weak tool edge is one of the causes that promoted flank wear. Therefore, further machining processes would not be effective, causing damage to the cutting tool's edge [33]. Similar wear morphology can be seen in this research as presented in Fig. 8 where abrasion detected and prologed abrasion on the tool tips caused tool fracture.

As a result of this condition, alteration to the range of the parameter used in this experiment is needed. A more significant gap in selecting cutting speed and the feed rate value can lead to a more significant result. Aside from that, the potential of the cutting speed to be increased further can be seen as the flank wear showing promising results with the decrement of wear. Increasing the range of the parameters will allow for optimum parameters to be obtained with the low value of flank wear on the ZTA-TiO_2-Cr_2O_3 ceramic cutting tool.

3.2 Crater Wear

Similar to the trend of flank wear, crater wear shows an increase with the increment of cutting speed and feed rate [18]. Fig. 9 illustrates the graph of crater wear versus cutting speed at different feed rates. As shown in the graph, the crater wear trend decreases to about 77–94% when the cutting speed is increased from 314 to 455 m/min. A similar trend can be seen in Fig. 10, where the decrement in flank wear value of about 16–73% occurred due to the increment in the feed rate from 0.10 to 0.15 mm/rev. Additionally, the highest value of crater wear for the ZTA-TiO_2-Cr_2O_3 ceramic cutting tool obtained is 21.91 mm^2 at the lowest cutting speed of 314 m/min with the lowest feed rate of 0.10 mm/rev. Meanwhile, the lowest value of crater wear obtained for the ZTA-TiO_2-Cr_2O_3 ceramic cutting tool is 0.45 mm^2 at the highest cutting speed of 4550 m/min with the highest feed rate of 0.15 mm/rev.

Fig. 11 shows the observation made for the crater wear at feed rate 0.15 mm/rev with different cutting speed from 314m/min to 455m/min proving the decrement of the crater wear with increment of the cutting speed. Meanwhile, Fig. 12 display the crater observation with increment of feed rate with identical trend of crater wear with increment of feed rate from 0.1 to 0.15 mm.rev.

This result is supported by a study where the wear of mixed Al_2O_3 resulted in the diffusion of the material of the workpiece within the secondary shear zone causing the crater wear to be more vulnerable to the cutting speed than alumina [13]. The fast movement of the chips could noticeably disintegrate the edge structure of the cutting tool, and because of the higher pressure on the edge, flaking can be seen as a result of the crater wear [8]. Furthermore, crater wear could also be affected by the factors that influenced the flank wear as well [34]. Flaking observed in this experiment at cutting speed 408m/min and feed rate 0.10 mm/rev presented in Fig. 13. Analyzing Fig. 13(a), the cutting edge area shows the initial crater area that later developed into the flaking when part of the cutting edge was disintegrated due to high pressure

during the machining process and creating a larger crater area on the cutting tool surface. As the machining continue, the chipping start to take place due to the weak tool cutting edge as shown in the SEM micrograph.

3.3 Chipping

During the machining process, disruption can occur given the overload of the mechanical shock, such as excessive wear on the tool, resulting in chipping. It began with the crack initiation on the tool surface and found along the cutting tool's edge, adjacent to the tip of the tool. The cracks later spread widely until the chipping area can be observed [35]. One of the factors causing the chipping is the sudden loss of the sharp cutting edge [36]. Fig. 14 shows the chipping area observed on the ZTA-TiO_2-Cr_2O_3 ceramic cutting tool when machining with the cutting speed of 314 m/min and feed rate of 0.10, 0.13, and 0.15 mm/rev. It can be observed that the chipping area became smaller with the increase of feed rate from 0.10 to 0.15 mm/rev. However, contrary to the result obtained in [18] where the chipping area increases when the feed rate is increased from 0.1 to 0.5 mm/rev. This could be due to the range of the feed rate is higher compared to the feed rate used in this experiment. Therefore, there is possibility for increment of feed rate for ZTA-TiO_2-Cr_2O_3 cutting tool from 0.15 mm/rev to higher value. The changes in the chipping area of the cutting tool are also not significant when the cutting speed is increased. This could be due to excess mechanical shock like increment in the feed rate that interrupts the turning operation. Also, the feed rate used in this experiment is much smaller compared to the feed rate value used [35]. This condition demonstrated that the feed rate range could be further increased to observe the optimum value.

Aside from that, the oxidation of the wear caused by the high temperature produced during the process might also be a cause that influenced the chipping area [37]. The oxidation wear observed on the surface of the ZTA-TiO_2-Cr_2O_3 cutting tool presented in Fig. 15.

Other observation on the overall parameters shows that the chipping appears at combination of low cutting speed and and low feed rate as tabulated in Table 3. As the cutting speed increased to 455 m/min, no chipping can be seen on the cutting tool edge. This condition influenced by the temperature increment during the machining which lead to softening effect on the work material [18]. This condition will decrease the high pressure on the tool edge as the cutting chips will flow easier and thus prevent the chipping on the cutting tool. This result can be related to the flank wear and crater wear as discussed previously where the result also agree with this condition. Apart from that, the softening effect also may leads to a much more stable machining and reduce the vibration in the machining process thus reduce the chipping on the cutting tool [11].

Table 3
Observation on chipping presence at different parameter combination.

Cutting Speed (m/min)	Feed rate (mm/rev)		
	0.1	0.13	0.15
314	√	√	√
361	√	√	x
408	√	x	x
455	x	x	x
		√	Chipping
		x	No Chipping

Although the cutting speed does not show significant changes is chipping area, nevertheless, it give effects in term of the chipping presence. This result also displays that selection of correct range of parameters is crucial to optimize the performance of the ceramic cutting tools.

3.4 Surface Roughness on the Machined Surface

During the machining operation, surface roughness is one of the crucial requirements. The surface roughness value can be influenced by many aspects, such as the cutting parameters, workpiece variables, and tool variables [6]. In this research, surface roughness was measured on the machined surface, stainless steel 316 L. Fig. 16 reflects the surface roughness; Ra of machined surface versus cutting speed at different feed rates. Based on the graph, the surface roughness trend decreases by about 56–78% when the cutting speed increases from 314 to 455 m/min. A similar trend can be seen in Fig. 17, where the decrement in surface roughness value of about 29–67% occurred due to the increment in feed rate from 0.10 to 0.15 mm/rev. Additionally, the highest value of surface roughness on the machined surface is 7.36 μm at the cutting speed of 314 m/min with a feed rate of 0.10 mm/rev. In contrast, the lowest value of surface roughness on the machined surface is 0.50 μm at the cutting speed of 455 m/min with a feed rate of 0.15 mm/rev.

Several studies can support this finding where the surface roughness on the machined surface decreases with an increase of the spindle speed [16][18][38]. This situation is due to the polishing effect occurring on the machined surface during the high-speed machining, resulting in better surface roughness [18]. Apart from that, the constancy of the cutting noise also affects the quality of the machined surface [16]. The high temperature on the cutting tool's tip caused by the high friction also explained the situation. However, the wear of the cutting tool would be higher given the increase in temperature [18].

Conclusions

Flank wear, crater wear, and chipping of the ZTA-TiO_2-Cr_2O_3 ceramic cutting tool and surface roughness of the machined surface, stainless steel 316L at different parameters was investigated in this work. The following conclusions are drawn based on the experimental investigations of this study:

- The flank wear of the ZTA-TiO_2-Cr_2O_3 ceramic cutting tool decreased when the cutting speed and feed rate increased. The lowest value of flank wear obtained is 0.044 mm at the highest cutting speed of 455 m/min and the highest feed rate of 0.15 mm/rev.
- The crater wear of the ZTA-TiO_2-Cr_2O_3 ceramic cutting tool decreased when the cutting speed and feed rate increased. The lowest value of crater wear obtained is 0.45 mm^2 at the highest cutting speed of 455 m/min and the highest feed rate of 0.15 mm/rev.
- The chipping area became smaller with the increase of feed rate from 0.10 to 0.15 mm/rev.
- The surface roughness of the machined surface, stainless steel 316L decreased when the cutting speed and feed rate increased. The lowest value of surface roughness on the machined surface is 0.50 μm at the highest cutting speed of 455 rpm and the highest feed rate of 0.15 mm/rev.

Declarations

Acknowledgment

The author would like to acknowledge the financial support from IIUM RMC Grant – (RMCG20-0031) and International Islamic University Malaysia where this research is conducted.

References

1. Grigoriev SN, Fedorov SV, Hamdy K. Materials, properties, manufacturing methods and cutting performance of innovative ceramic cutting tools – a review. Manuf Rev. 2019;19:6.
2. Li L, Li Y, Development and trend of ceramic cutting tools from the perspective of mechanical processing. IOP Conf. Series: Earth and Environmental Science 2017, 94: 012062.
3. Yin, Z, Huang C, Yuan J, et al. Cutting performance and life prediction of an Al_2O_3/TiC micro–nano-composite ceramic tool when machining austenitic stainless steel. Ceram 2015, 41:5, 7059–7065.
4. Wang D, Zhao J, Cao Y, et al. Wear behavior of an Al_2O_3/TiC/TiN micro-nano-composite ceramic cutting tool in high-speed turning of ultra-high-strength steel 300 M, Int. J. Adv. Manuf. Technol. 2016, 87: 3301–3306.
5. Wang D, Xue C, Cao Y, et al., Fabrication and cutting performance of an Al_2O_3/TiC/TiN ceramic cutting tool in turning of ultra-high-strength steel. Int. J. Adv. Manuf. Technol. 2017, 91: 5–8, 1967–1976.
6. Nandhakumar S, Prakash RS. Parametric optimization in CNC turning of martensitic stainless steel 416 using Taguchi method, J. Chem. Pharm. Res. 2017: 974–2115.

7. Islam MW, Bakhtierkhalzi M, Suzauddin M, et al. Influences of various ceramic oxides on physical and mechanical properties of zirconia toughened alumina (ZTA): A review. International Conference on Mechanical, Industrial, and Materials Engineering 2017.
8. Bakar HA, Fahmi N, Mokhtar F, et al. Fabrication and machining performance of powder compacted alumina-based cutting tool. MATEC Web of Conferences 2018, 150: ISSN: 2261-236X.
9. Mohamad NA, Ratnam MM, Chipping detection in ceramic insert during turning by analysis of workpiece surface profile using cross-correlation. IOP Conference Series: Materials Science and Engineering 2019, 530: 1,1757-899X.
10. Lee WK, Ratnam MM, Ahmad ZA In-process detection of chipping in ceramic cutting tools during turning of difficult-to-cut material using vision-based approach, Int. J. Adv. Manuf. Technol. 2016, 85: 5–8, 1275–1290.
11. Khan AA, Mohiuddin AKM, Norhamzan NH, A comparative study on flank wear of ceramic and tungsten carbide inserts during high speed machining of stainless steel. Int. J. Appl. Eng. Res. 2018, 13: 2541–2544.
12. Azhar AZA, Choong IC, Mohamed H, et al. Effects of Cr_2O_3 addition on the mechanical properties, microstructure, and wear performance of zirconia-toughened-alumina (ZTA) cutting inserts. J. Alloys Compd. 2012, 513: 91–96.
13. Varma BS, Kumar SS, Devi, RS, Behavior and Wear Mechanisms of ZTA Based Ceramic Cutting Tools on Hardened Steels, Int. J. Appl. Eng. Res. 2016, 6: 4, 8–14.
14. Szutkowska M, Fracture toughness of advanced alumina ceramics and alumina matrix composites used for cutting tool edges. J. Achiev. Mater. Manuf. Eng. 2012, 54:2, 201–210.
15. Manshor H., Azhar AZA, Abd Rashid R, et al. Effects of Cr_2O_3 addition on the phase, mechanical properties, and microstructure of zirconia-toughened alumina added with TiO_2 (ZTA–TiO_2) ceramic composite. Int. J. Refract. Hard. Met. 2016, 61: 40–45.
16. Singh BK, Mondal B, Mandal N, Machinability evaluation and desirability function optimization of turning parameters for Cr_2O_3 doped zirconia toughened alumina (Cr-ZTA) cutting insert in high-speed machining of steel. Ceram. 2016, 42:2, 3338–3350.
17. Sabuan NA, Zolkafli N, Mebrahitom A, Azhari A, Mamat O. (2018). The development of Zirconia and Coppertoughened Alumina ceramic insert. IOP Conference Series: Materials Science and Engineering, 342(1), 012106.
18. Ali AM, Hamidon NE, Zaki NKM, Mokhtar S, Azhar AZA, Bahar R. Ahmad ZA, The effect of cutting parameters on the performance of ZTA-MgO cutting tool. IOP Conference Series: Materials Science and Engineering 2018, **290**:1.
19. Rejab NA, Azhar AZA, Ratnam MM et al. The effects of CeO_2 addition on the physical, microstructural, and mechanical properties of yttria stabilized zirconia toughened alumina (ZTA). Int. J. Refract. Hard. Met. 2013, 36: 162–166.

20. Verma V, Kumar BM, Synthesis, microstructure, and mechanical properties of $Al_2O_3/ZrO_2/CeO_2$ composites with addition of nickel and titania processed by conventional sintering. Materials Today: Proceedings, 2017, 4:2, 3062-3071.
21. Manshor H, Aris SM, Azhar AZA, et al. Effects of TiO_2 addition on the phase, mechanical properties, and microstructure of zirconia-toughened alumina ceramic composite. Ceram 2015, 41:3, 3961–3967.
22. Dhar SA, Shuvo SN, Rashid AKMB, Mechanical and microstructural properties of TiO_2 doped zirconia toughened alumina (ZTA) ceramic composites at different TiO_2 contents. Am. J. Eng. Res. 2015, 4:11, 8–12.
23. Song J, Huang C, Lv M, et al. Cutting performance and failure mechanisms of TiB2-based ceramic cutting tools in machining hardened Cr12MoV mold steel. Int. J. Adv. Manuf. Technol. 2014, 70:1-4, 495–500.
24. Lima FF, Sales WF, Costa ES, et al. Wear of ceramic tools when machining Inconel 751 using argon and oxygen as lubri-cooling atmospheres. Ceram. 2017, 43:1, 677–685.
25. Tan DW, Guo WM, Wang HJ, et al. Cutting performance and wear mechanism of TiB_2-B_4C ceramic cutting tools in high speed turning of Ti_6Al_4V alloy. Ceram. 2018, 44:13, 15495–15502.
26. Cheng M, Liu H, Zhao B, et al. Mechanical properties of two types of Al_2O_3/TiC ceramic cutting tool material at room and elevated temperatures. Ceram. 2017, 43:16, 13869–13874.
27. Azhar AZA, Mohamad H., Ratnam MM, et al. The effects of MgO addition on microstructure, mechanical properties and wear performance of zirconia-toughened alumina cutting inserts. J. Alloys Compd. 2010, 497:1-2, 316–320.
28. Mondal B, Mandal N, Doloi B, Development of Ce-PSZ-/Y-PSZ-Toughened Alumina Inserts for High-Speed Machining Steel. Int. J. Appl. Ceram. Technol. 2014, 11:2, 228–239.
29. Manshor H, Abdullah EC, Azhar AZA, et al. Microwave sintering of zirconia-toughened alumina (ZTA)-TiO_2-Cr_2O_3 ceramic composite: The effects on microstructure and properties. J Alloys Compd. 2017;722:458–66.
30. Milak PC, Minatto FD, Montedo ORK, Wear performance of alumina-based ceramics-a review of the influence of microstructure on erosive wear. Cerâmica 2015, 61:357, 88–103.
31. Kamely MA, Noordin MY, Ay BH, et al. The performance of low cost cutting tools when machining hardened steel of 60 HRC. J. Adv. Manuf. Technol. 2012, 6:1.
32. Suresh R, Basavarajappa S, Samuel GL, Some studies on hard turning of AISI 4340 steel using multilayer coated carbide tool. Meas. 2012, 45:7, 1872–1884.
33. Fatin MRN, Hadzley ABM, Izamshah R, et al. An Experimental Study of Wear Mechanism on High Speed Machining of FC300 Gray Cast Iron Using TiAlN Coated Carbide Cutting Tool. Appl. Mech. Mater. 2015, 761:257–261.
34. Kumar AS, Durai AR, Sornakumar T, Wear behaviour of alumina based ceramic cutting tools on machining steels. Tribol. Int. 2006, 39: 3, 191–197.

35. Deng J, Wu F, Lian Y, Xing Y, et al. Erosion wear of CrN, TiN, CrAlN, and TiAlN PVD nitride coatings. Int. J. Refract. Hard. Met. 2012, 35, 10–16.
36. Sultan AZ, Sharif S, Kurniawan D, Effect of machining parameters on tool wear and hole quality of AISI 316L stainless steel in conventional drilling. Procedia Manuf. 2015, 2: 202–207.
37. Wang Y, Yan X, Li B, et al. The study on the chip formation and wear behavior for drilling forged steel S48CS1V with TiAlN-coated gun drill, Int. J. Refract. Hard. Met. 2012, 30:1, 200–207.
38. Ali AM, Abdullah NS, Ratnam MM, et al. Linear shrinkage of the ZTA ceramic cutting inserts. Procedia Chem. 2016;19:879–83.

Figures

Figure 1

ZTA-TiO2-Cr2O3 cutting tool

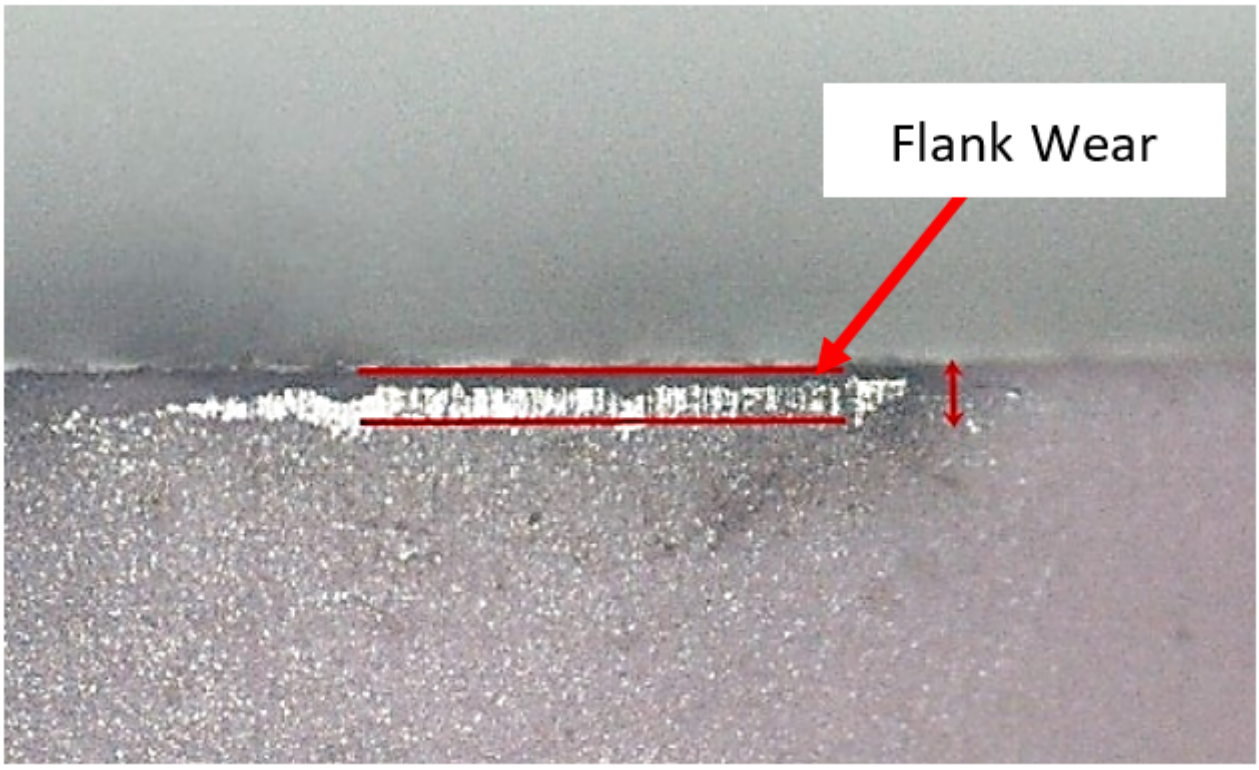

Figure 2

The flank wear measured in this experiment

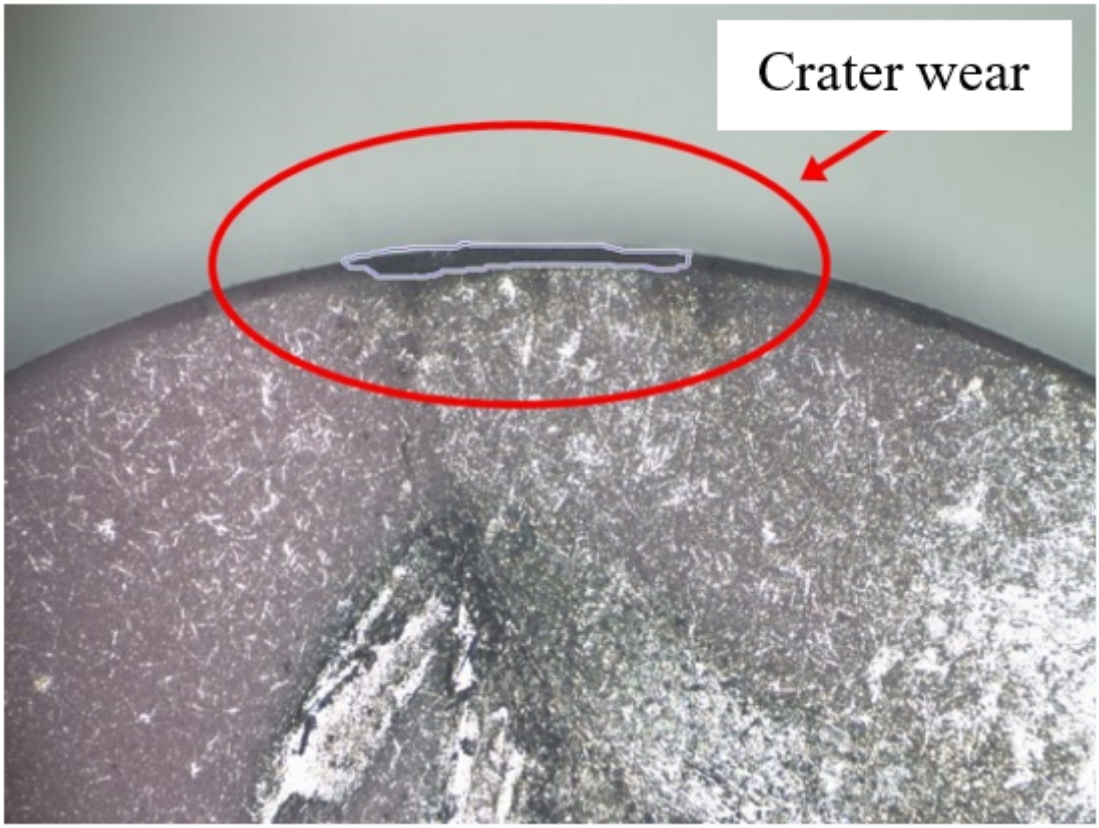

Figure 3

The crater wear observed in the experiment

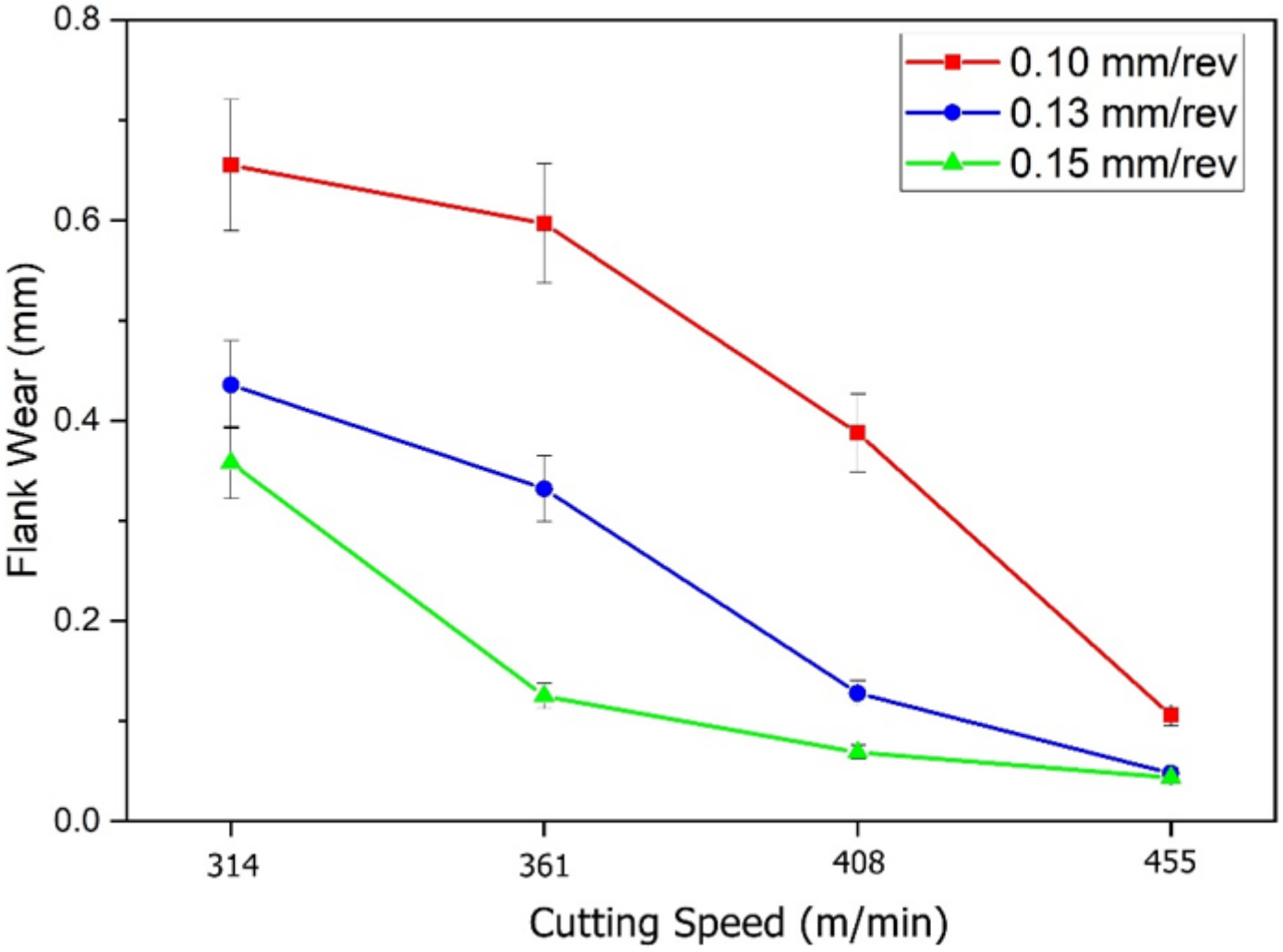

Figure 4

Graph of flank wear (mm) vs. cutting speed (m/min) at different feed rate (mm/rev).

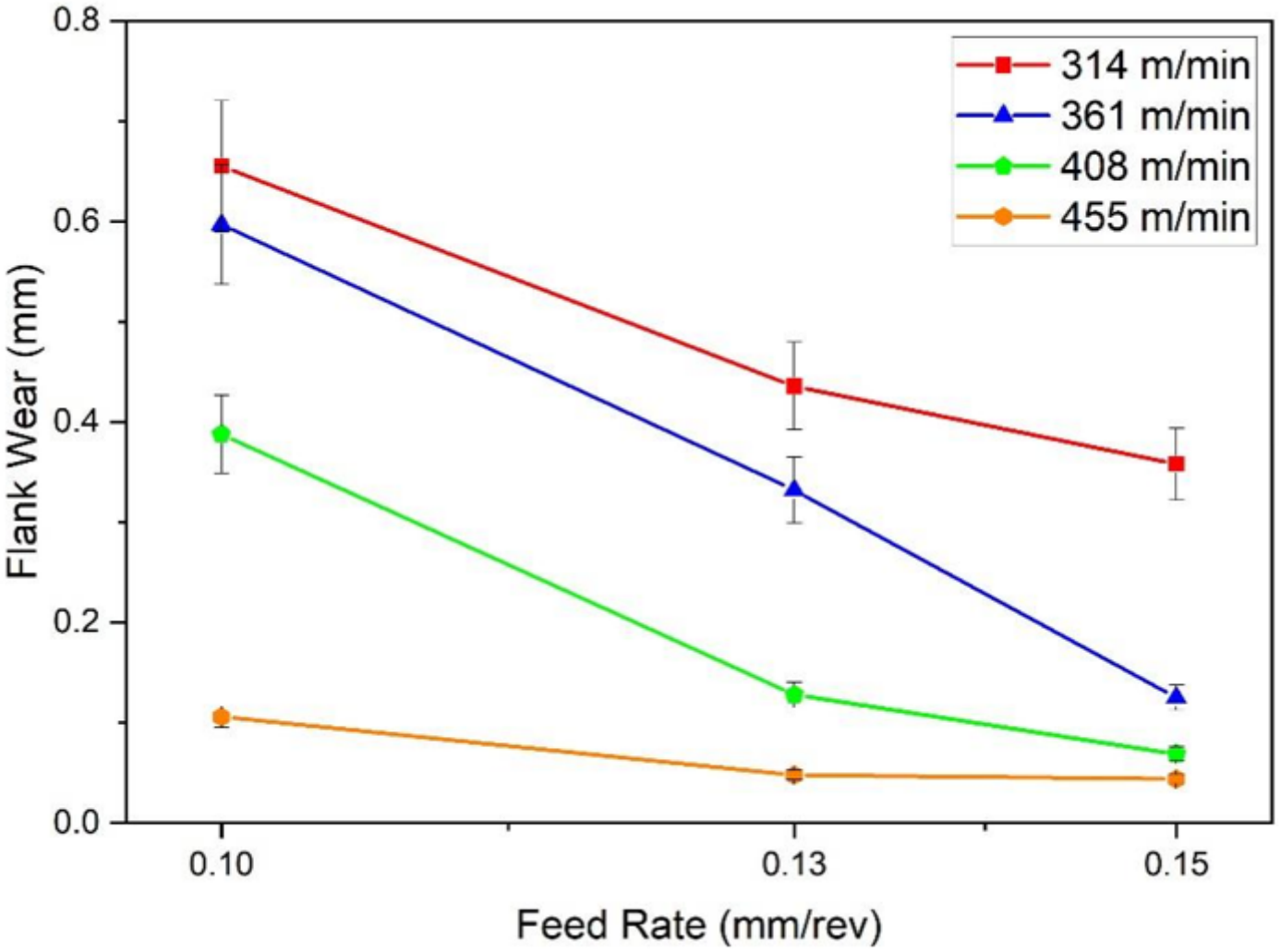

Figure 5

Graph of flank wear (mm) vs. feed rate (mm/rev) at different cutting speed (m/min).

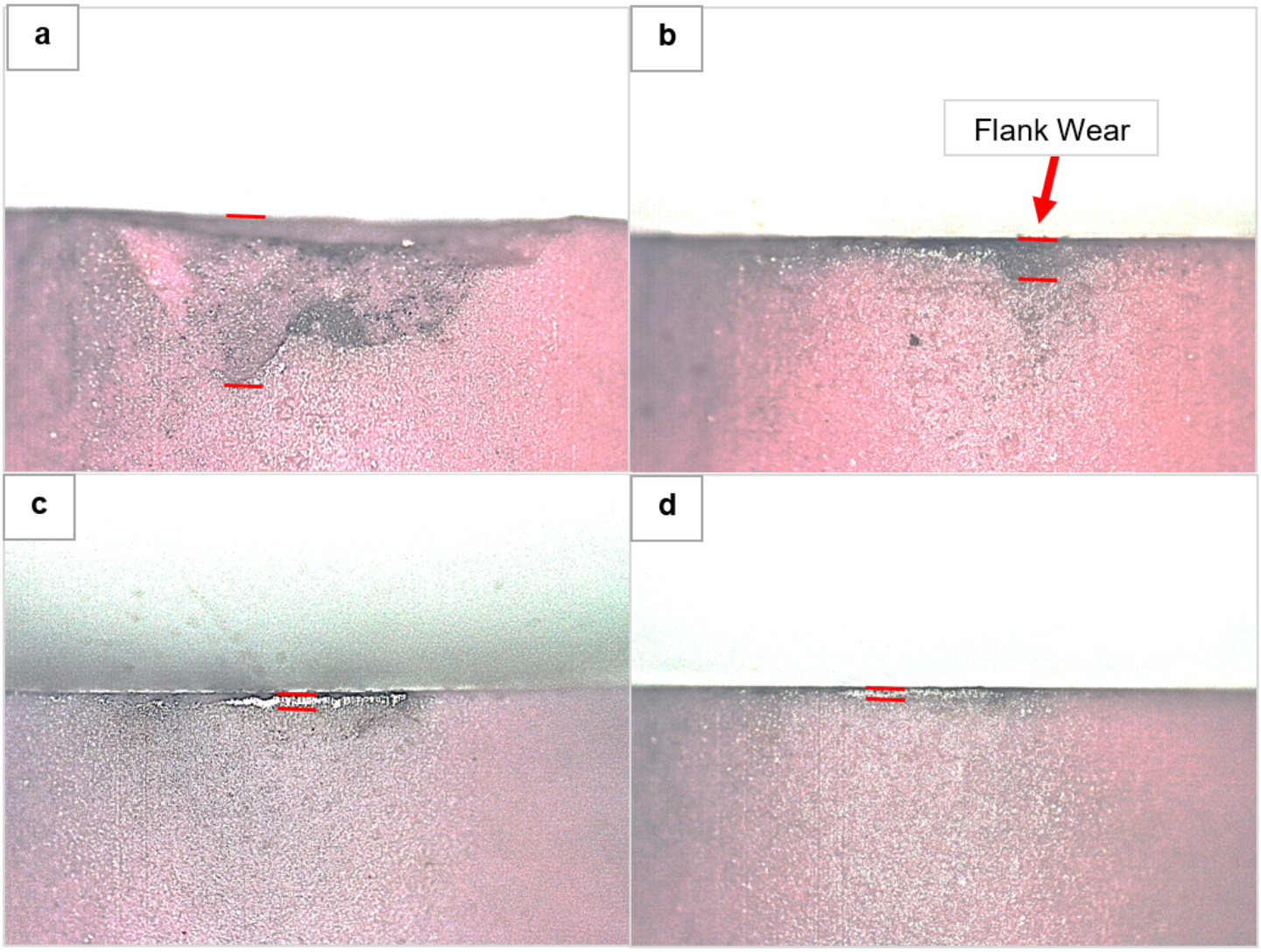

Figure 6

Flank wear at feed rate 0.15mm/rev and cutting speed (a) 314 m/min (b) 361 m/min and (c) 408 m/min and d) 455 m/min

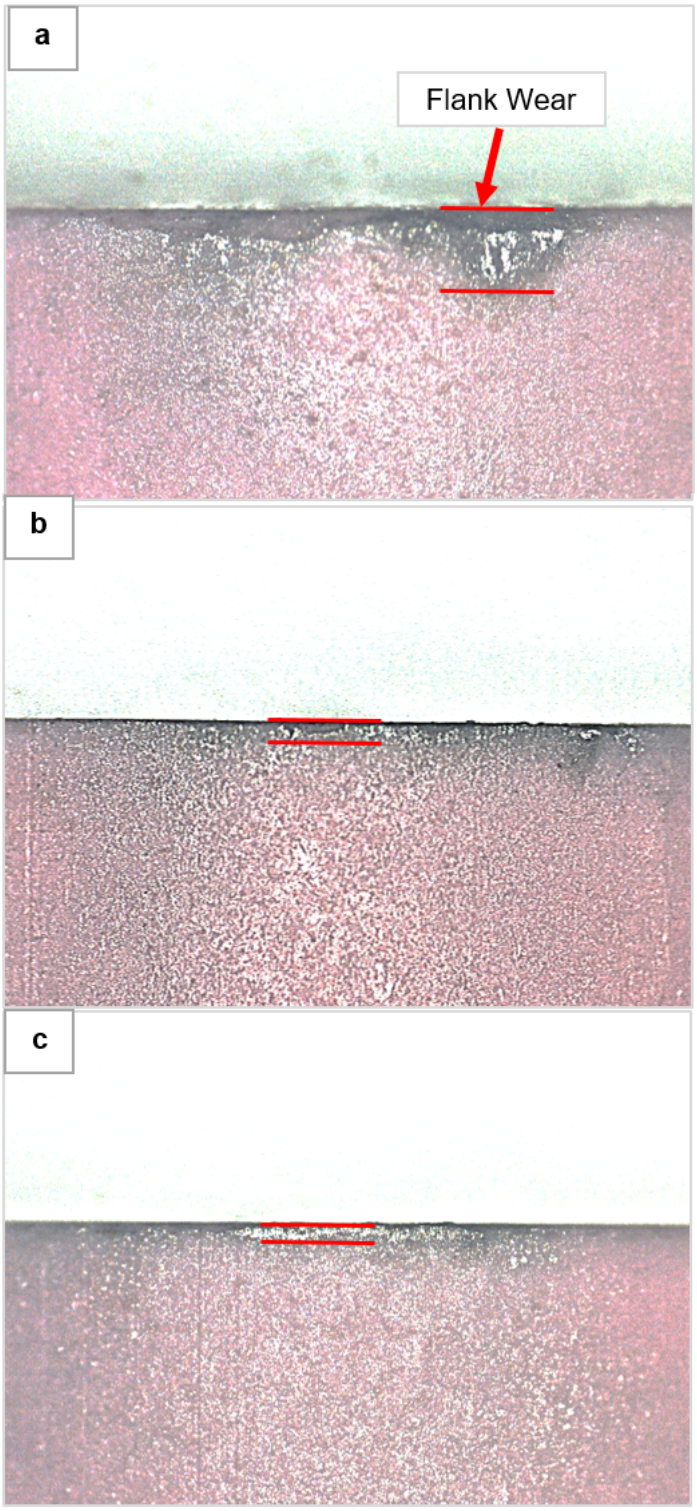

Figure 7

Flank wear at cutting speed 455 m/min and feed rate (a) 0.1 mm/rev, (b) 0.13 mm/rev and (c) 0.15 mm/rev

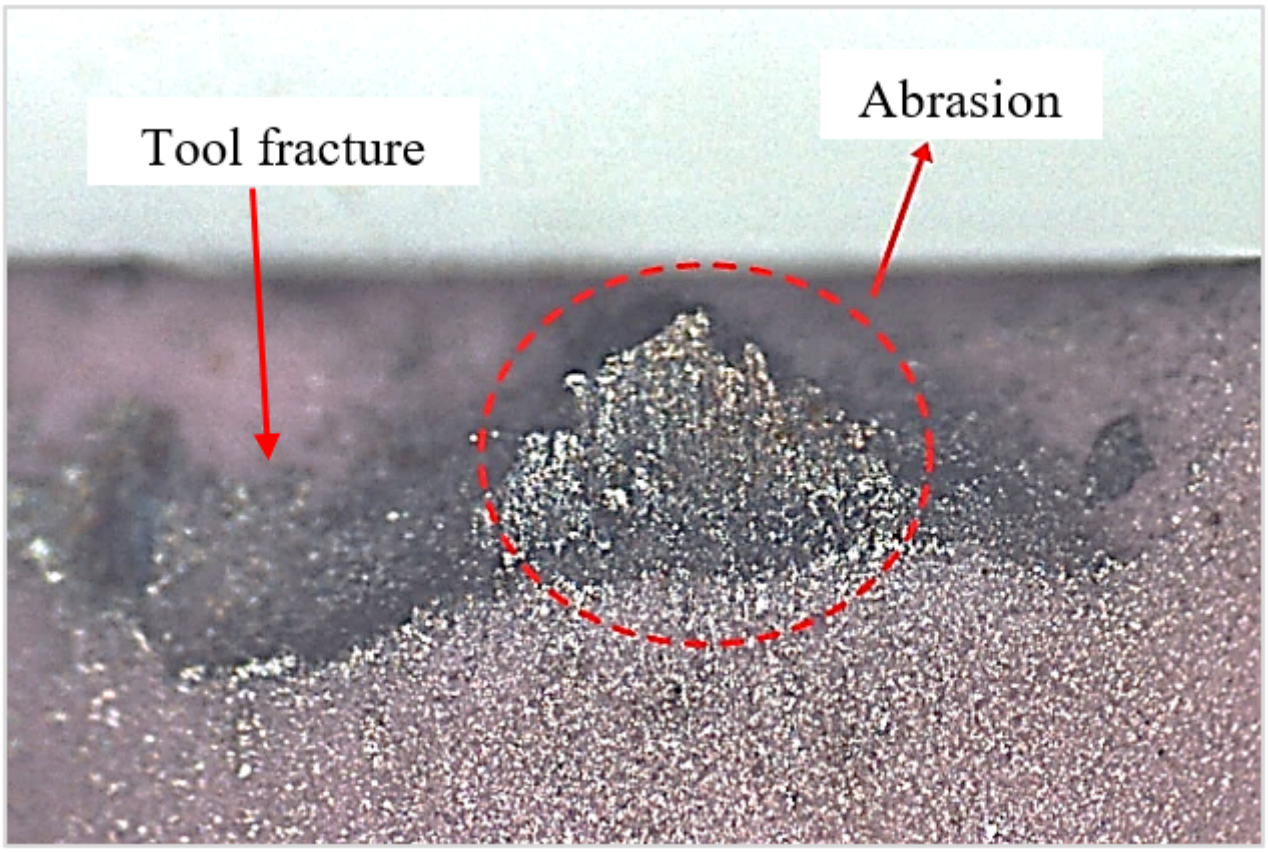

Figure 8

ZTA-TiO2-Cr2O3 cutting tool wear morphology at cutting speed of 361 m/min and feed rate of 0.10 mm/rev.

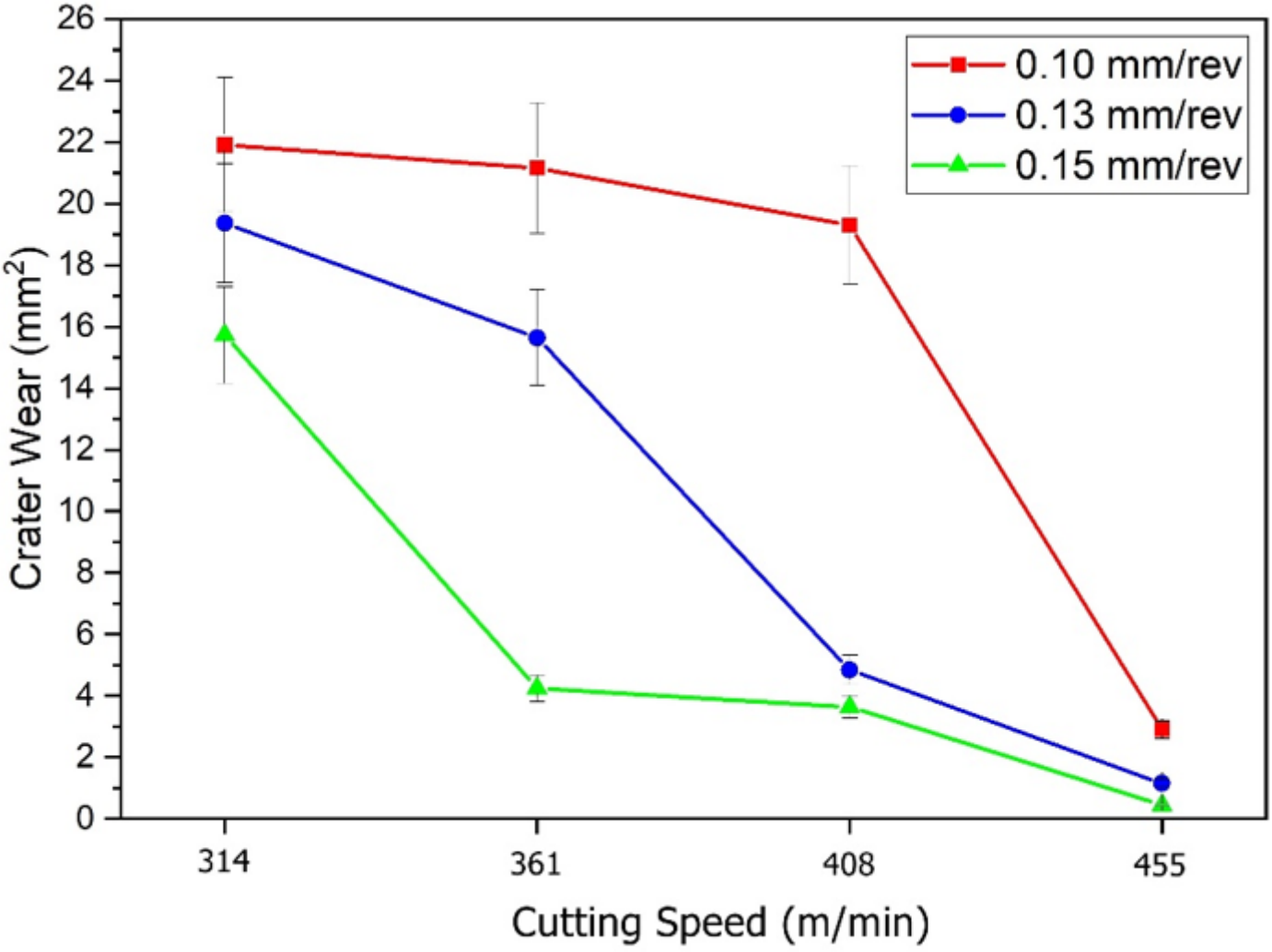

Figure 9

Graph of crater wear (mm2) vs. cutting speed (m/min) at different feed rate (mm/rev).

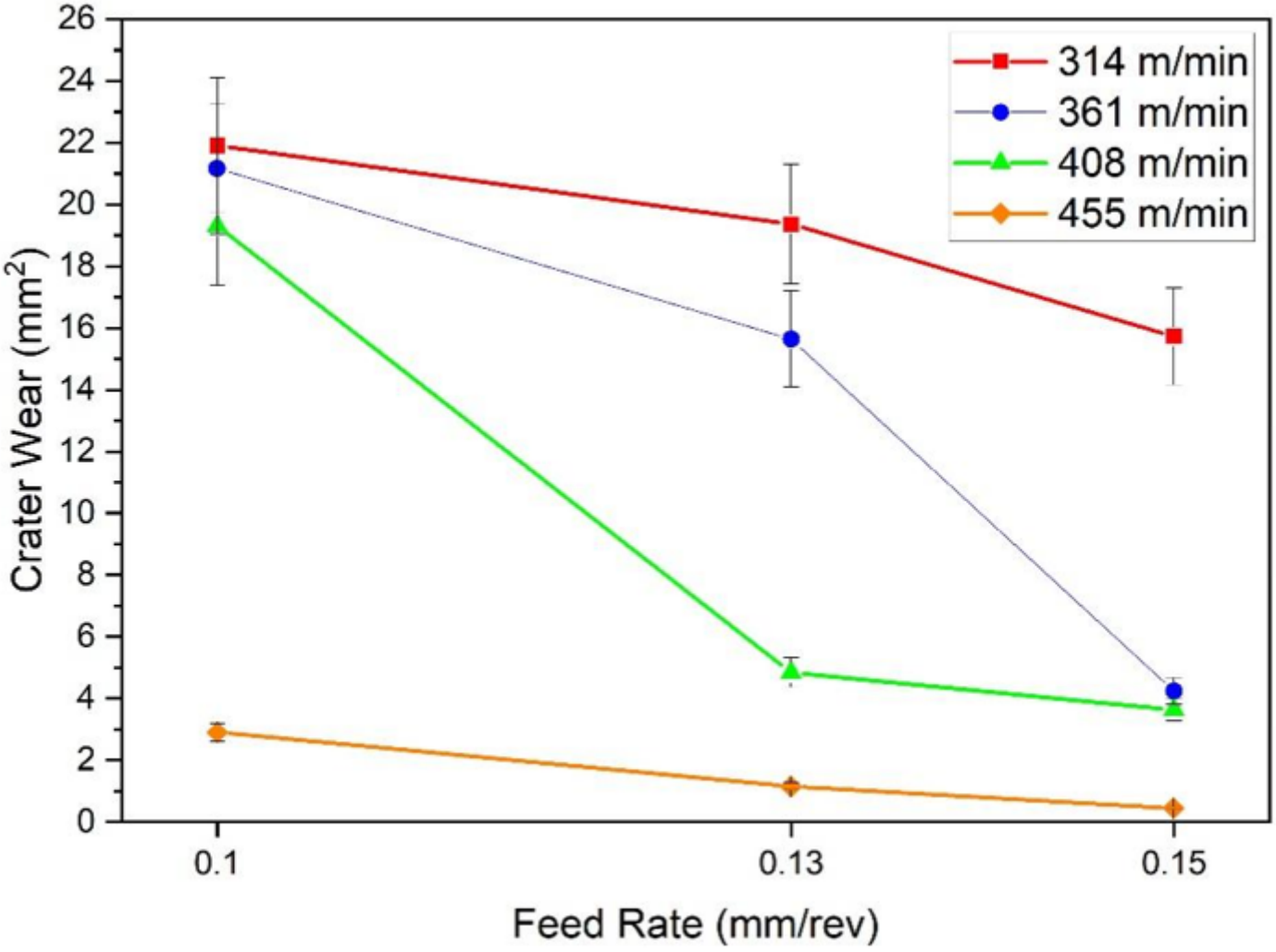

Figure 10

Graph of crater wear (mm2) vs. feed rate (mm/rev) at different cutting speed (m/min).

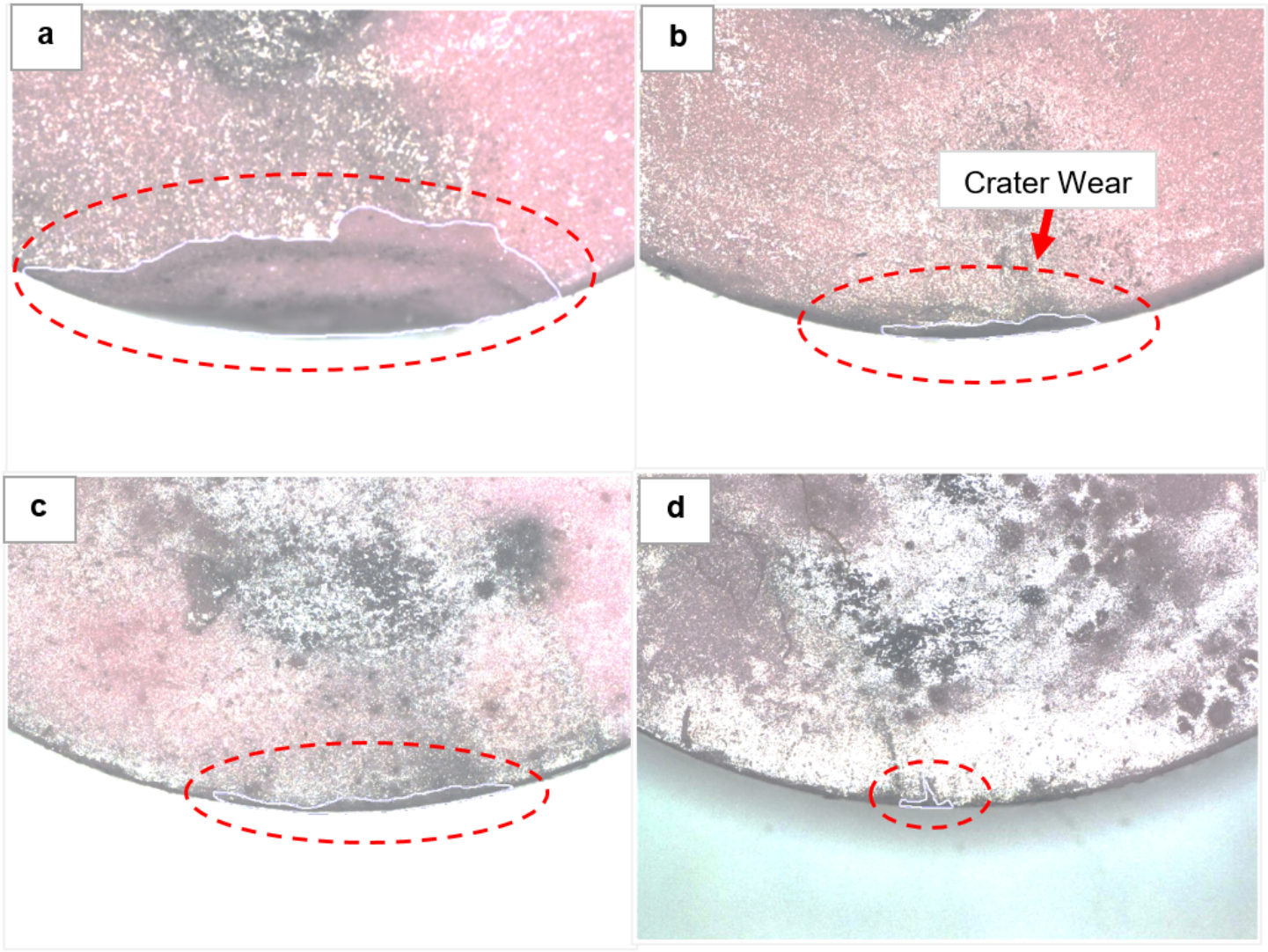

Figure 11

Crater wear at feed rate 0.15mm/rev and cutting speed (a) 314 m/min (b) 361 m/min and (c) 408 m/min and d) 455 m/min

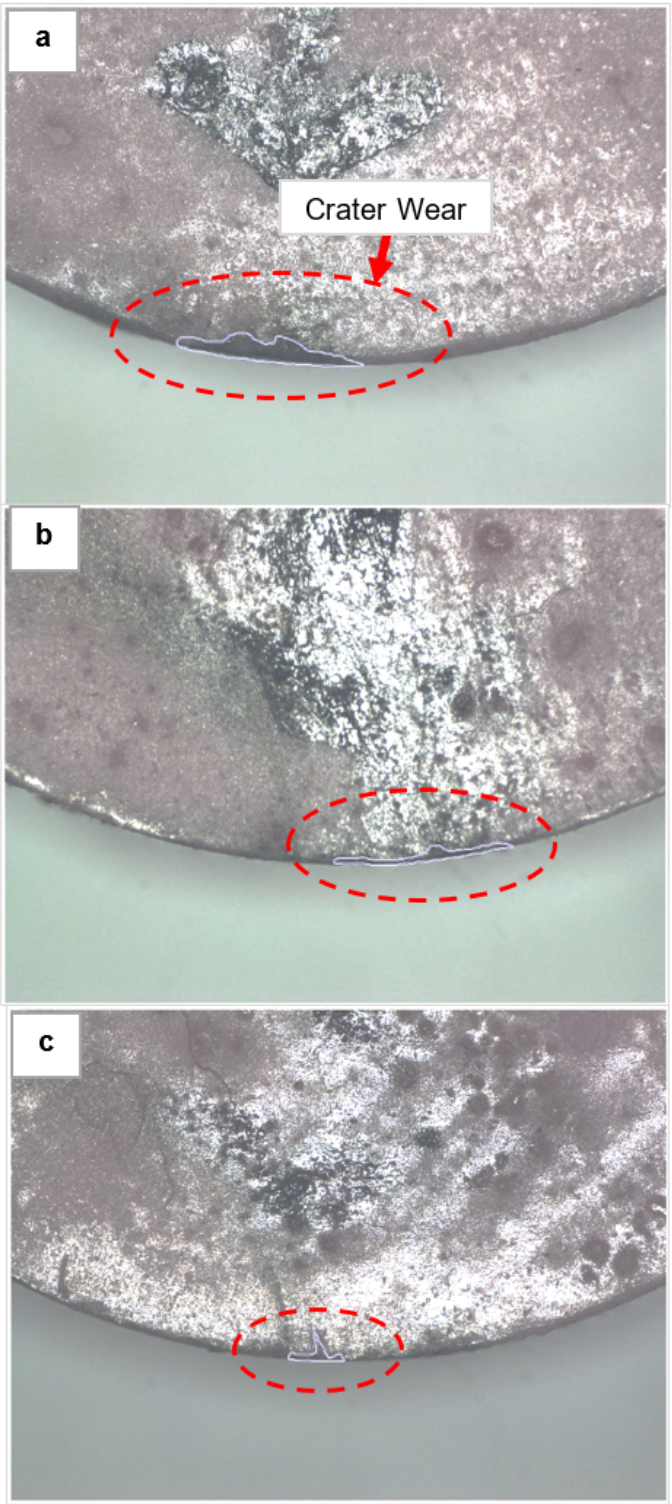

Figure 12

Crater wear at cutting speed 455 m/min and feed rate (a) 0.1 mm/rev, (b) 0.13 mm/rev and (c) 0.15 mm/rev

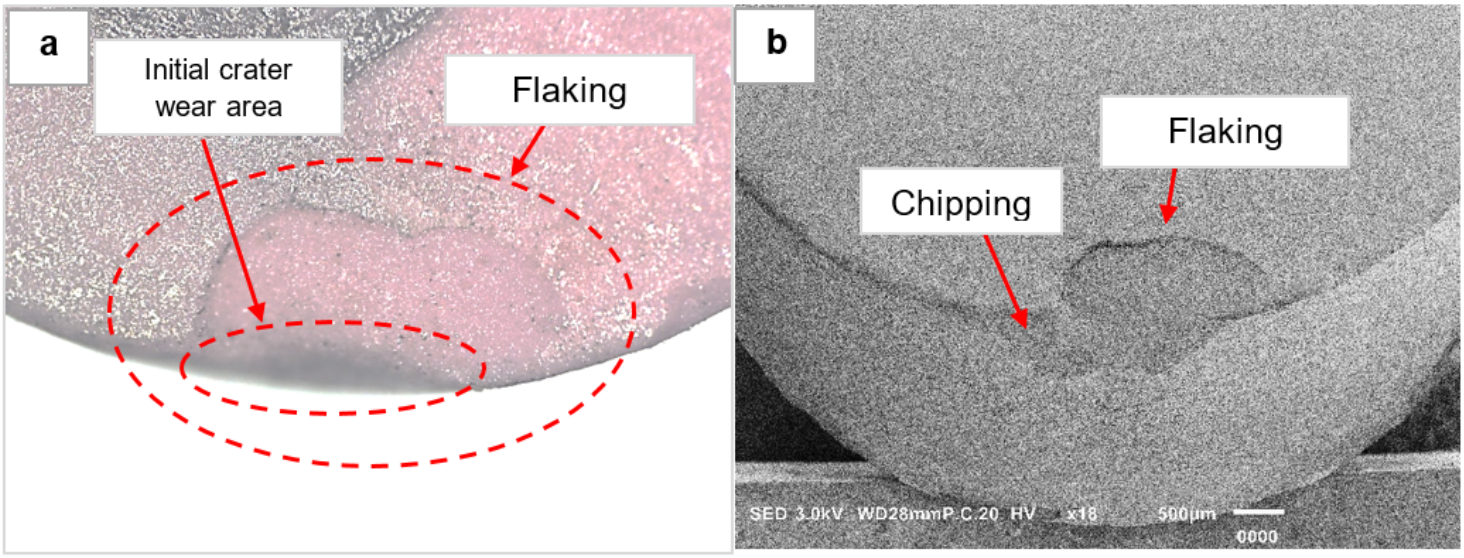

Figure 13

ZTA-TiO2-Cr2O3 cutting tool wear morphology at cutting speed of 408 m/min and feed rate of 0.10 mm/rev (a) under the optical microscope (b) under the SEM.

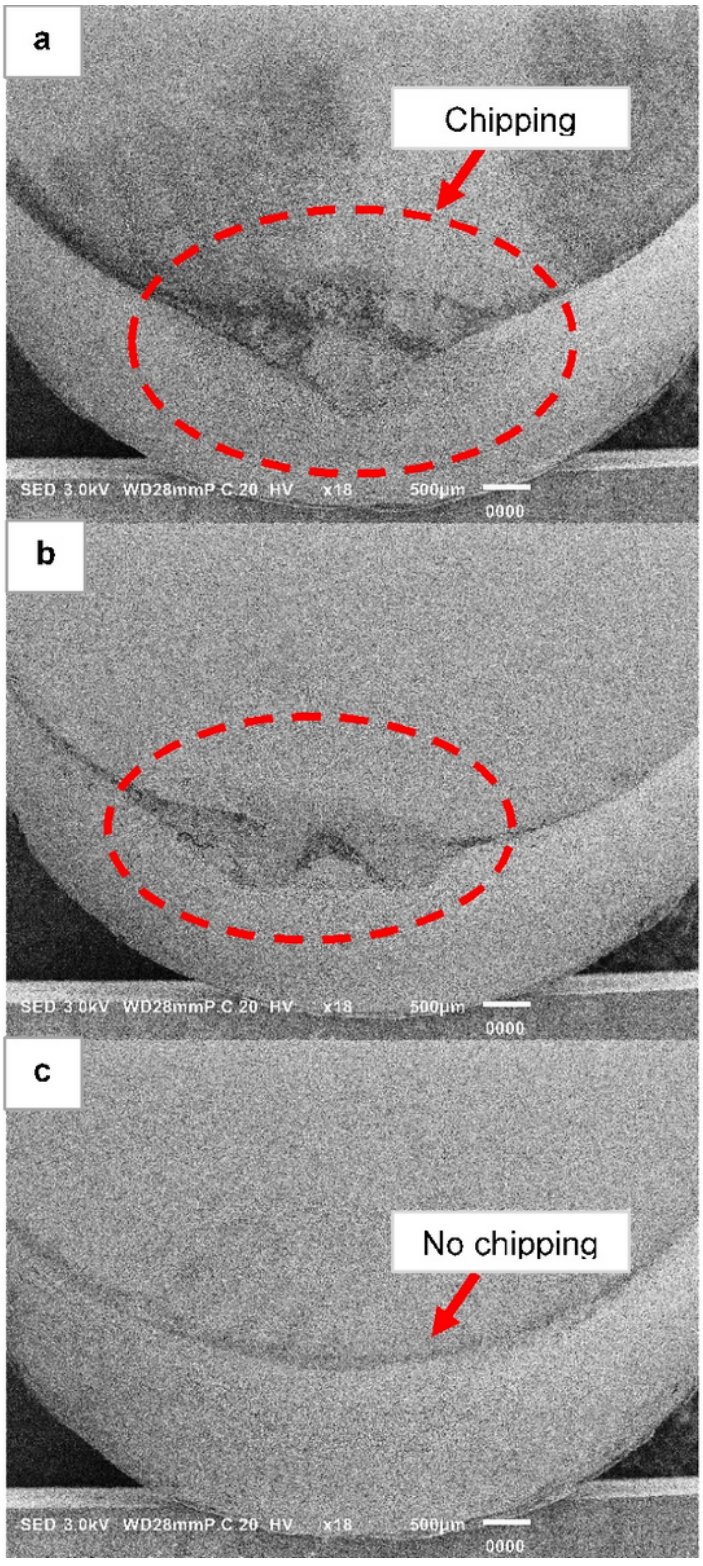

Figure 14

Chipping images of ZTA-TiO2-Cr2O3 ceramic cutting tool with cutting speed of 361 m/min and feed rate of (a) 0.1 mm/rev (b) 0.13 mm/rev (c) 0.15 mm/rev.

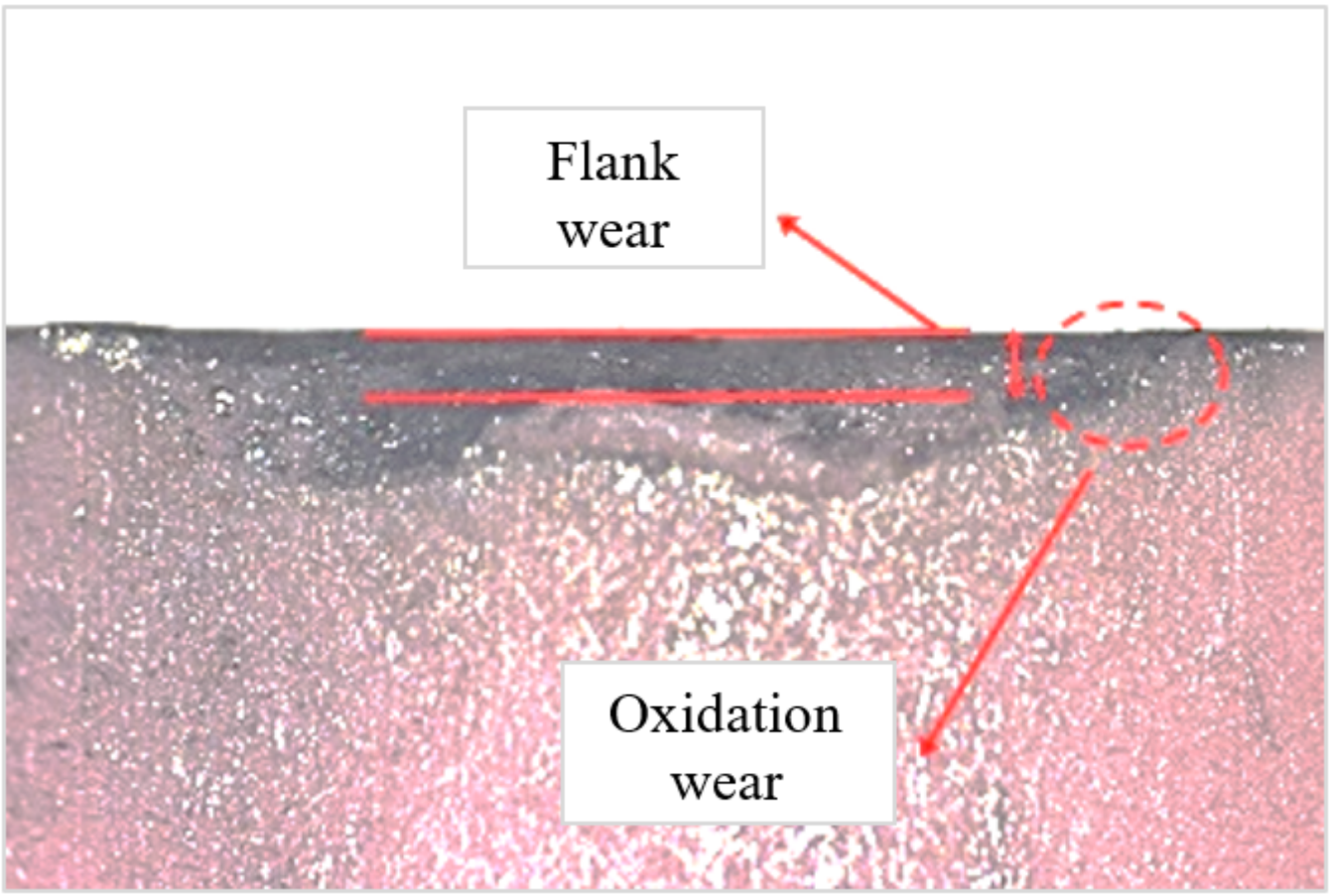

Figure 15

ZTA-TiO2-Cr2O3 cutting tool wear morphology at cutting speed of 314 m/min and feed rate of 0.13 mm/rev.

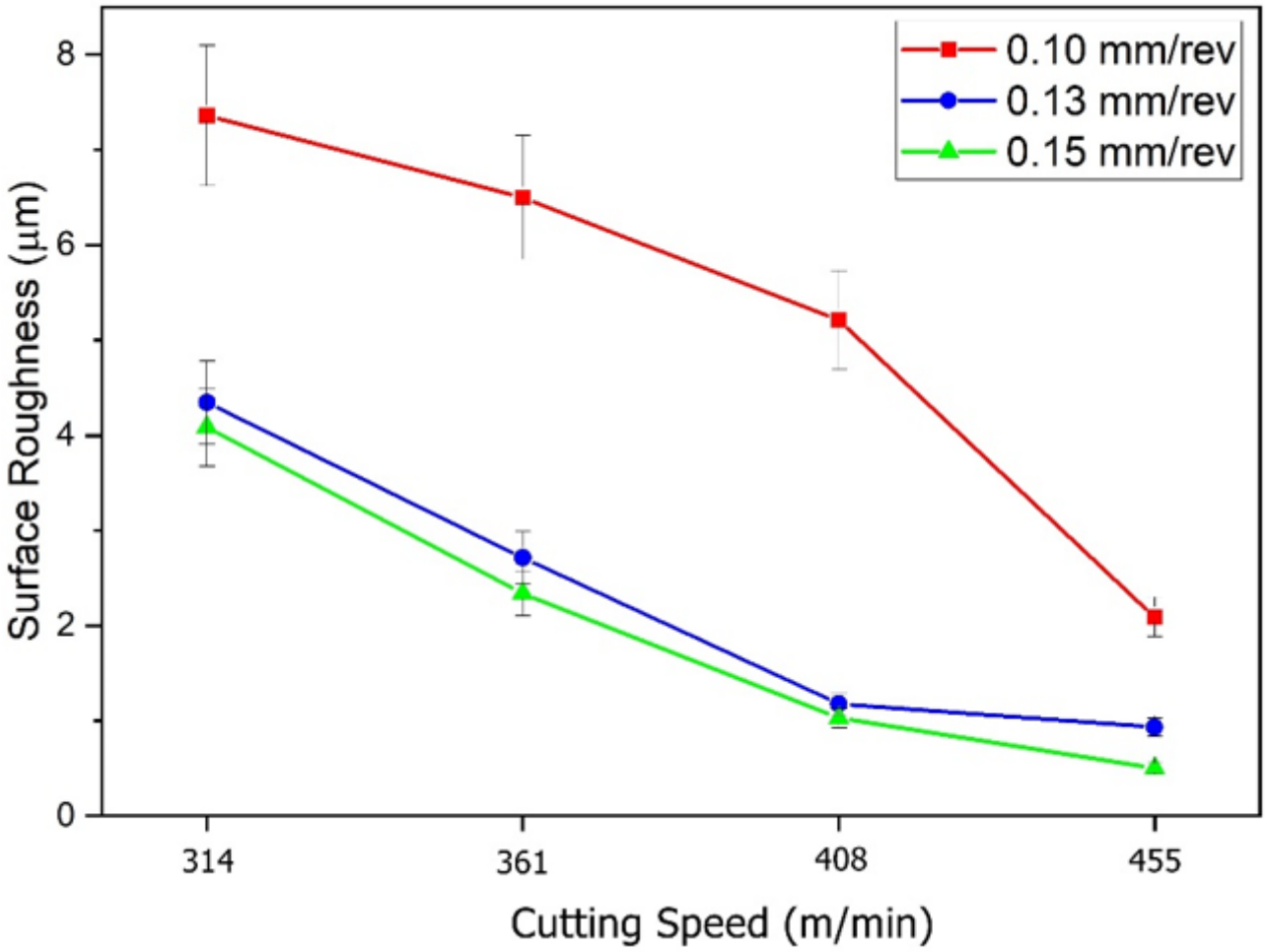

Figure 16

Graph of surface roughness (µm) vs. cutting speed (m/min) at different feed rate (mm/rev).

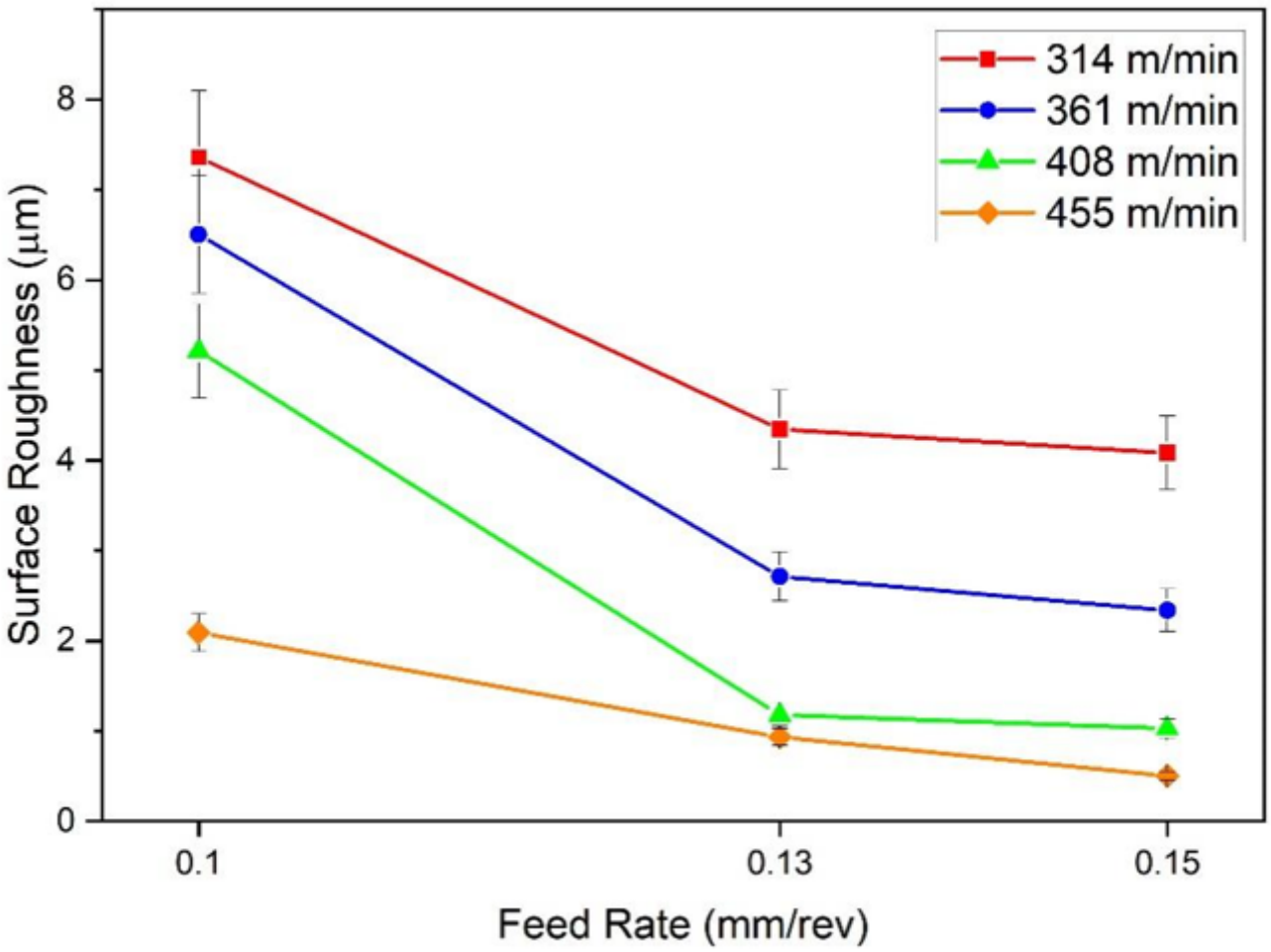

Figure 17

Graph of surface roughness (µm) vs. cutting speed (m/min) at different feed rate (mm/rev).